Applied Surface Science 357 (2015) 1225–1230

Contents lists available at ScienceDirect

Applied Surface Science

journal homepage: www.elsevier.com/locate/apsusc

Surface damage and mechanical properties degradation of Cr/W multilayer films irradiated by Xe^{20+}

Feida Chen [a], Xiaobin Tang [a,b,*], Hai Huang [a], Jian Liu [a], Huan Li [a], Yunlong Qiu [c], Da Chen [a,b]

[a] Department of Nuclear Science & Engineering, Nanjing University of Aeronautics and Astronautics, Nanjing, China
[b] Jiangsu Key Laboratory of Nuclear Energy Equipment Materials Engineering, Nanjing, China
[c] ZhongXing Energy Equipment Co., Ltd., Haimen, China

ARTICLE INFO

Article history:
Received 10 June 2015
Received in revised form 21 August 2015
Accepted 20 September 2015

Keywords:
Cr/W multilayer
Xe ions irradiation
Grain growth
Swelling
Nano-indentation

ABSTRACT

3 MeV Xe^{20+} ion irradiation experiments were performed on the Cr/W multilayer films to investigate the evolution of surface morphology and mechanical properties. Results showed that the W layer in the as-deposited pure W and Cr/W multilayer films are simple cubic structure, but it is not stable under ions irradiation. After exposure to 2.14×10^{18} m^{-2} Xe ions irradiation, the W layer has completely transformed into the bcc structure. For surface morphology characterization, serious swelling effects were observed in the pure W films. Compared with the pure W films, the Cr/W multilayer films showed much better resistance against the irradiation-induced swelling. Meanwhile, the decrease of hardness and Young's modulus of the Cr/W multilayer films was also less than the pure W films. Results of surface morphology and mechanical tests suggested that radiation tolerance of the Cr/W multilayer films is significantly better than the pure W films.

1. Introduction

The nano-scaled metallic multilayer composites show excellent self-healing performance against irradiation damage and provide possible novel designs of ultrahigh radiation tolerant materials. At present, these composites are regarded as potential structural materials in the next generation of nuclear reactor systems [1,2]. The majority of previous studies focused on fcc/bcc multilayer systems such as Cu/Nb [3], Ag/V [4], Cu/W [5], Cu/Fe [6], and Ni/Fe [7] because the large lattice parameter mismatch of fcc/bcc interfaces enhances defect storage capability of multilayers [8]. Unfortunately, when high neutron-induced radioactivity is considered, a few fcc metals could be applied in nuclear reactors. In this work, a novel Cr/W multilayer thin film was presented. The Cr/W multilayer system was selected because of the following reasons: (i) both Cr and W are low-level neutron activation radioactive elements that are widely used in structural materials; (ii) despite having the same crystal structure, the lattice parameter mismatch between Cr (2.88 Å) and W (3.16 Å) is large enough to absorb radiation-induced defects [9]; (iii) the Cr/W system can form immiscible and thermostable interfaces because its mixing enthalpy is +1 kJ/mol according to the Miedema model [9,10].

During a long-term service in extreme irradiation environments, distinct crystallinity modification and property degradation could occur in the materials because of the accumulation of radiation-induced point defects. Charged xenon ion implantation has been widely used as a more secure and effective method of introducing high radiation damage to samples in a short time without any risk of radiation. Since Xe ions are chemically inert to the materials, the crystallinity modification and property degradation of materials can simply owe to the accumulation of vacancies and interstitials, which is caused by atomic-displacement cascades [11].

In this work, surface morphology change and mechanical property degradation of the Cr/W multilayer films are reported. Based on the magnetron sputtering technique, two kinds of Cr/W multilayer films with different modulation periods were prepared and irradiated by 3 MeV Xe^{20+} ions in fluences ranging from 4.3×10^{17} ions/m^2 to 1.07×10^{19} ions/m^2. Comparisons of the microstructure and mechanical properties of as-deposited and post-irradiation samples provide important insights on the evaluation of enhanced radiation tolerance in immiscible multilayer systems.

2. Experimental details

Pure W films and two kinds of Cr/W multilayer films with different modulation periods were prepared for subsequent irradiation experiments. Cr/W multilayer films were deposited by RF

* Corresponding author at: Department of Nuclear Science & Engineering, Nanjing University of Aeronautics and Astronautics, Nanjing, China.
E-mail address: tangxiaobin@nuaa.edu.cn (X. Tang).

http://dx.doi.org/10.1016/j.apsusc.2015.09.170
0169-4332/

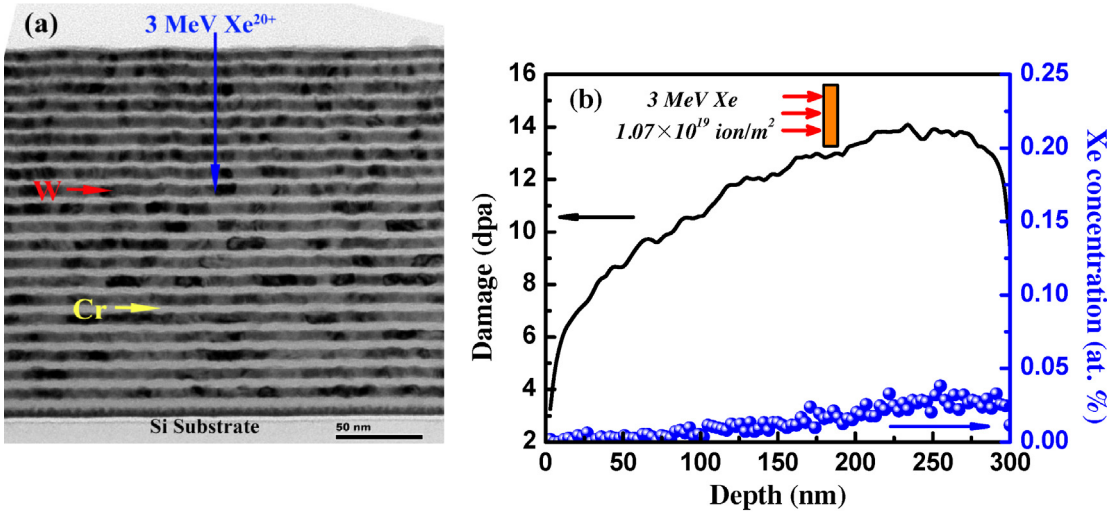

Fig. 1. The film samples were irradiated by 3 MeV Xe^{20+} ions: (a) the low-magnification transition electron microscopy photograph of the cross section of the as-deposited $[Cr/W(5\,nm)]_{20}$ multilayer film. The dark regions are the W layer and the bright regions are the Cr layers; (b) the damage profiles and Xe concentration distribution in the Cr/W multilayer.

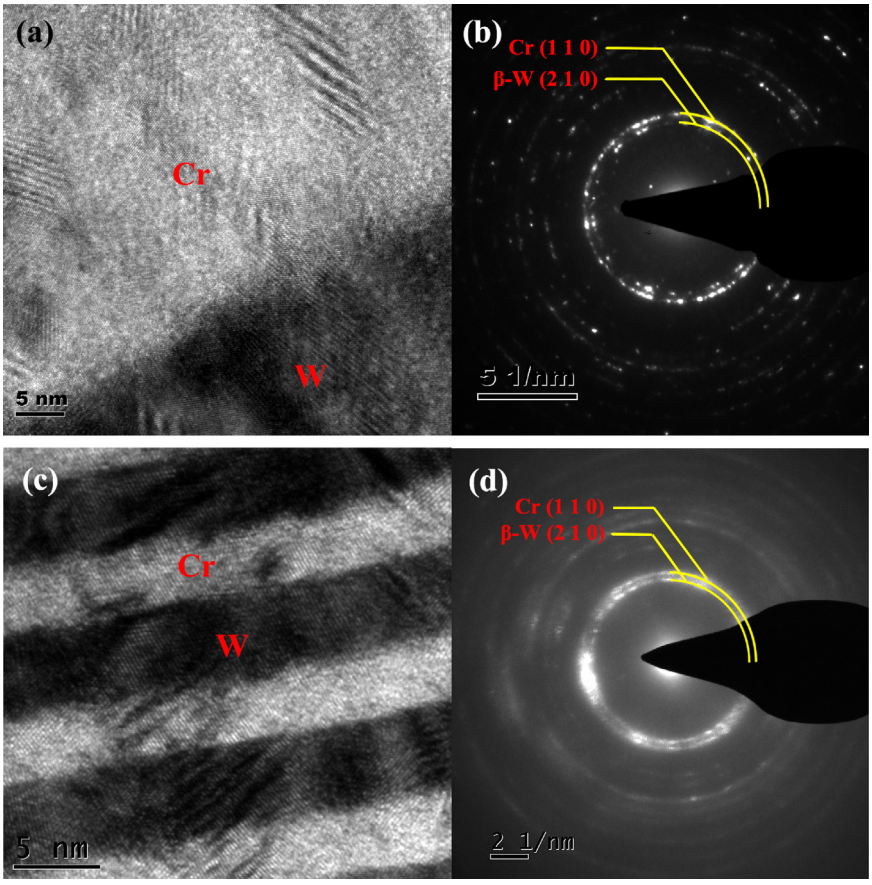

Fig. 2. The high resolution cross section TEM image and corresponding selected area electron diffraction pattern of the as-deposited $[Cr/W\,(50\,nm)]_2$ and $[Cr/W\,(5\,nm)]_{20}$ multilayer thin films: (a) the HRTEM image of the as-deposited $[Cr/W(50\,nm)]_2$ multilayer film; (b) the SAED pattern of the as-deposited $[Cr/W(50\,nm)]_2$ multilayer film; (c) the HRTEM image of the as-deposited $[Cr/W(5\,nm)]_{20}$ multilayer film and (d) the SAED pattern of the as-deposited $[Cr/W(5\,nm)]_{20}$ multilayer film.

magnetron sputtering in a high-vacuum system. The base pressure of the system was evacuated to less than 2×10^{-4} Pa and the Ar gas pressure during deposition was 0.3 Pa. Cr (99.95 at.%) and W (99.95 at.%) targets were used in the experiments. Every target was 76 mm in diameter and 3 mm in thickness, while the Si (1 0 0) single crystal substrate was 50 mm in diameter. The sputtering power of Cr and W was 175 W, and the deposition rates of Cr and W were 2 Å/s and 1.5 Å/s, respectively. During deposition, the Si substrate was kept rotating at room temperature to achieve a uniform thickness. The single Cr and W layers within the Cr/W multilayer films have equal layer thickness that vary from 5 nm to 50 nm, whereas the total thickness of each film was approximately 200 nm. After

deposition, 5 mm × 5 mm square pieces were cut apart from the Si substrate using a laser from the back side of the substrate to avoid damaging the films.

Xenon irradiation experiments were performed on the 320 kV-platform at the Institute of Modern Physics, Chinese Academy of Sciences (CAS). The film samples were irradiated by 3 MeV Xe^{20+} ions in a fluence ranging from 4.3×10^{17} ions/m^2 to 1.07×10^{19} ions/m^2 at room temperature (shown in Fig. 1(a)). During irradiation, the beam current was approximately 0.95 μA, and the beam area was 17 mm × 17 mm. The samples were separated into two groups. The films in the first group were all-area irradiated, whereas the other group was half-area irradiated. The relationship between ion fluence and material damage degree was determined using the full-damage cascade mode of SRIM2013 [12]. The displacement threshold energies for Cr and W in the simulation were set to be 28.0 and 44.0 [13], respectively. As shown in Fig. 1(b), displacement damage increases with the film depth, varying from 3 dpa to 13 dpa when Xe irradiation fluence reaches 1.07×10^{19} m^{-2}. Most of the Xe ions penetrate away from the thin films, thus, the Xe concentration within the films was very low. Displacement damage effects are introduced by Xe irradiation.

The crystal structure of the pre- and post-irradiated film samples was identified by X-ray diffraction (XRD, Rigaku Dmax 2500V) and transition electron microscopy (TEM, Tecnai G2 F20 S-Twin). Grazing incidence X-ray diffraction (GIXRD) with Cu K_α radiation ($\lambda = 0.154$ nm) was carried out with the incident angle fixed at 1°. Surface morphology characterizations (AFM, Veeco Nanoscope 3D) of the irradiated films were performed on the all-area irradiated samples, whereas height characterizations were finished on the half-area irradiated samples.

Nano-indentation tests (Nano Indenter G200, Agilent) were performed using the continuous stiffness measurement method [14] with a Berkovich tip. To obtain the entire range of the hardness/modulus–depth curve from the thin film to the substrate, we set the maximum indentation depth at 1000 nm and took the peak value as hardness/modulus of films. Five indentation tests were performed on each sample to determine hardness and modulus.

3. Results and discussion

3.1. Microstructure

Fig. 2(a) and (b) shows the HRTEM image and the corresponding SAED pattern of the as-deposited [Cr/W (50 nm)]$_2$ film. They indicate that both the Cr layer and W layer are polycrystalline. The radii of the 1st and 2nd diffraction ring in Fig. 2(b) are 4.432 1 nm^{-1} and 4.902 1 nm^{-1} respectively, which match β-W (2 1 0) and Cr (1 1 0) planes. For the as-deposited [Cr/W (5 nm)]$_{20}$ film, its HRTEM image and SAED pattern (shown in Fig. 2(c) and (d)) show that it also has the polycrystalline structure and the interfaces between Cr and W layers are sharp.

Fig. 3 shows the X-ray diffraction curves of the three species of thin films: pure W film, [Cr/W (50 nm)]$_2$ film, and [Cr/W (5 nm)]$_{20}$ film. In Fig. 3(a), the as-deposited pure W film appears like a pure simple cubic lattice type polycrystalline film. The two peaks at 35.5° and 40° represent the β-W (2 0 0) crystal faces and β-W (2 1 0) crystal faces, respectively [15]. However, the β phase tungsten seems unstable under the Xe ions irradiation. After 4.3×10^{17} m^{-2} Xe ion irradiation, the β-W (2 0 0) peak disappears gradually and the β-W (2 1 0) peak shifts to 40.2° apparently. Since the peak at 40.2° represents α-W (1 1 0), it indicates that the initial simple cubic structure began to transform into the bcc structure. According to Fig. 3(a), the simple cubic structure has completely transformed into the bcc structure at the medium ion fluence, 2.14×10^{18} m^{-2}.

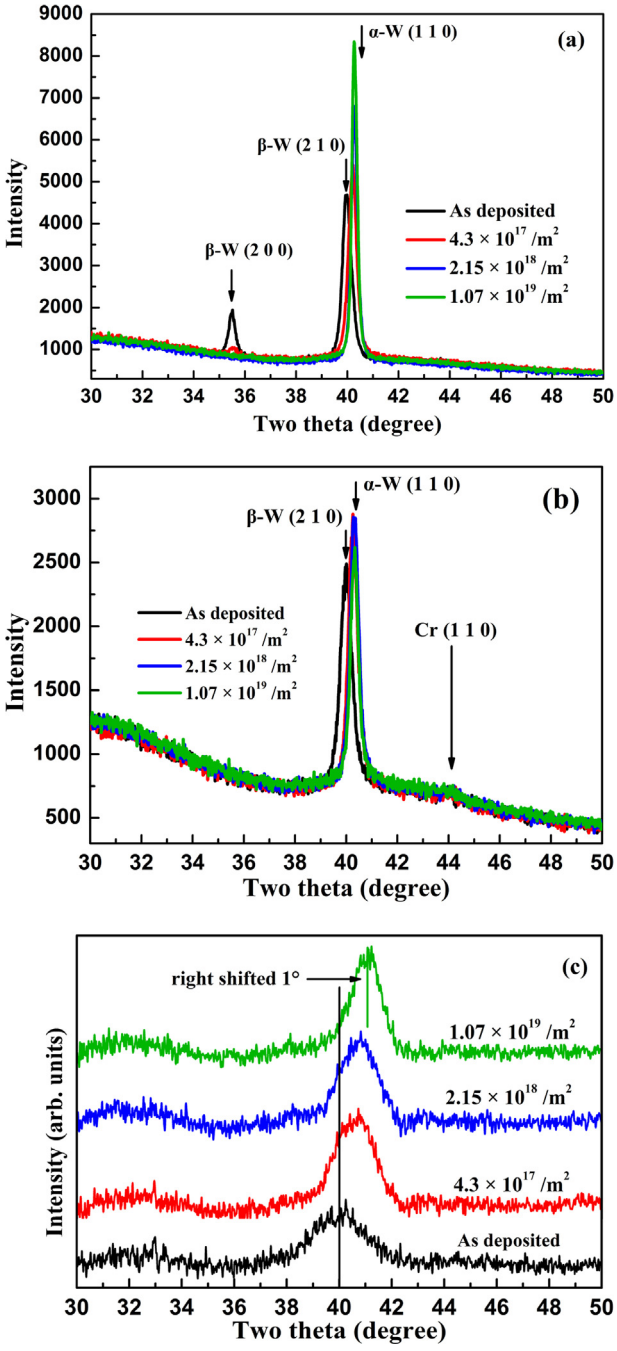

Fig. 3. Evolution of film structure after Xe ion irradiation: (a) pure W films; (b) [Cr/W (50 nm)]$_2$ multilayer films and (c) [Cr/W (5 nm)]$_{20}$ multilayer films.

The simple cubic structure to bcc structure transition of tungsten can also be observed in the post-irradiated [Cr/W (50 nm)]$_2$ and [Cr/W (5 nm)]$_{20}$ films. As shown in Fig. 3(b), the β-W (2 1 0) peak can be identified in the as-deposited multilayers while the β-W (2 0 0) peak is absence. This phenomenon is consistent with the SAED pattern we observed in Fig. 2(b). From Fig. 3(b), the right shift of β-W (2 1 0) peak is also evident after the least Xe ion irradiation (4.3×10^{17} m^{-2}). It seems that the multilayer structure does not work to prevent the phase transition. On the other hand, the Cr (1 1 0) peak which supposed to be at 44.4° can hardly be identified from all curves, even though its diffraction ring in SAED pattern (shown in Fig. 2(b)) is distinct. Hence, the detailed information about the structure change of Cr is uncertain still.

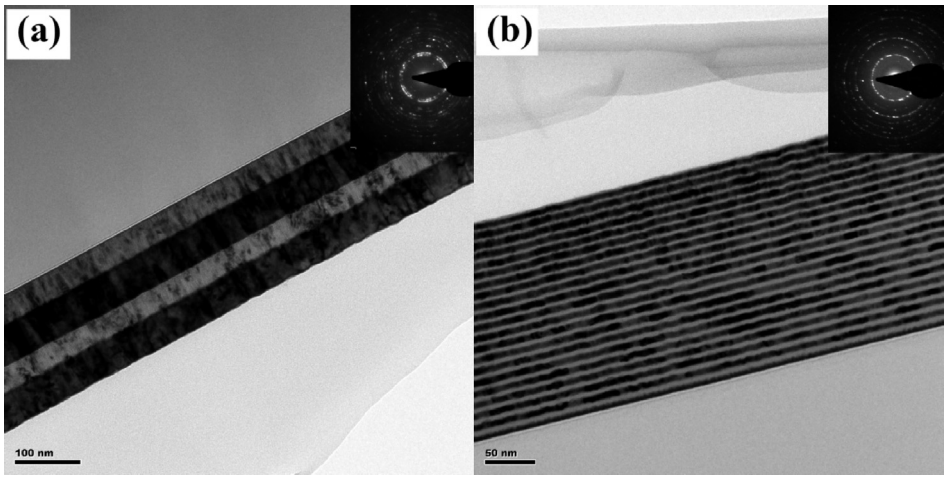

Fig. 4. Cross sectional TEM images of two species of Cr/W multilayer films upon 1.07×10^{19} m^{-2} Xe ion irradiation: (a) [Cr/W (50 nm)]$_2$ multilayer films; (b) [Cr/W (5 nm)]$_{20}$ multilayer films.

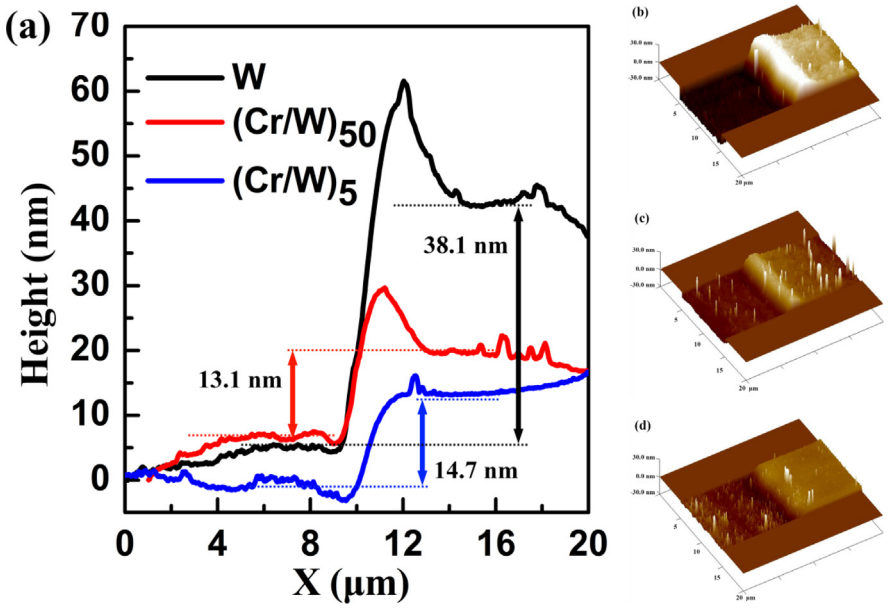

Fig. 5. Radiation-induced swelling effects on the three species of films upon 1.07×10^{19} m^{-2} Xe ion irradiation: (a) height difference between the irradiated and un-irradiated regions. The curves are presented after averaging along the *y* axis; (b) 3D morphology of the half-area irradiated pure W film. The left region is the un-irradiated region; (c) the [Cr/W (50 nm)]$_2$ multilayer film and (d) the [Cr/W (50 nm)]$_2$ multilayer film.

As shown in Fig. 3(c), the peak intensity of the [Cr/W (5 nm)]$_{20}$ multilayer films is significantly weaker than the other two films. The peaks are quite broad, indicating nanosize grains. After 4.3×10^{19} m^{-2} ion fluence irradiation, the β-W (2 1 0) peak shifts from 40° to 41° gradually while its shape changes slightly. Since the α-W (1 1 0) peak is at 40.2°, the peak at 41° is quite strange. Although some peaks belonging to chromium oxides are near 41°, but they are not the main peak and the highest diffraction peaks of these chromium oxides are absence in the curve. So oxidization is not a reasonable explanation. On the other hand, N. Durand et al. have reported that W thin films prepared by magnetron sputtering have strong compressive residual stresses. Under ion irradiation condition, these stresses can be relaxed quickly. Stress relaxation effect may explain the shift of the peak [16]. Combined with the SRIM simulation referred above, the experiment results indicate that phase transition of tungsten under ion irradiation at room temperature happened in all the three thin films. For [Cr/W (5 nm)]$_{20}$ multilayers, its grain keeps nanometer size under ions irradiation and defects produced by irradiation can be restored via lattice constant distortion.

The cross sectional TEM images of the two post-irradiated Cr/W multilayer films are shown in Fig. 4. Interfaces in both multilayer films remained sharp even after 1.07×10^{19} m^{-2} Xe ion irradiation (12 dpa). The continuous dense SAED pattern in Fig. 4(b) indicates that the [Cr/W (5 nm)]$_{20}$ multilayer films are mainly composed of nanocrystals. This phenomenon is consistent with the XRD study results described above.

3.2. Surface morphology

To further study the swelling effects of films, the researchers performed an AFM measurement on the half-area irradiated samples. Fig. 5 indicates that the height difference between the irradiated and un-irradiated regions can reach dozens of nanometers, although the film's total thickness is only 200 nm. Meanwhile, the two species of Cr/W multilayer films have greater radiation

Table 1
Roughness on scanning square areas of 10 μm × 10 μm for the as-deposited and post-irradiated films.

Materials	Roughness (nm Rms)	
	As-deposited	1.07×10^{19} m^{-2}
Pure W films	3.226	2.923
$[Cr/W(50\,nm)]_2$	1.768	1.595
$[Cr/W(5\,nm)]_{20}$	1.537	0.884

tolerance than pure W films. However, the layer thickness-dependent of ΔH is absent in our study because the swelling height of the $[Cr/W\ (50\,nm)]_2$ multilayer film and the $[Cr/W\ (5\,nm)]_{20}$ multilayer film is very close.

The evolution of film roughness upon Xe ion irradiation was also performed on the all-area irradiated films by AFM. As shown in Table 1, the roughness of the as-deposited pure W films is the highest among the three species of as-deposited films. After irradiation, the roughness of all the three films decreases. The detailed surface morphology observations are presented in Fig. 6.

Fig. 6(a) shows that the size of hill-like particles formed on the pure W films are approximately 2 μm. The 3D morphology of these particles is distinct even when the height scale was set to 30 nm. The swelling phenomenon is supposed to be the main reason for the decreasing of films roughness. Similar phenomenon can be observed in the post-irradiated $[Cr/W\ (50\,nm)]_2$ multilayer films (Fig. 6(d)). Meanwhile, the $[Cr/W\ (5\,nm)]_{20}$ multilayer film is so flat that the height scale was set to 6 nm to clearly show its morphology. The changes of surface morphology between the as-deposited sample (Fig. 6(e)) and post-irradiated sample (Fig. 6(f)) are significantly smaller than the two films.

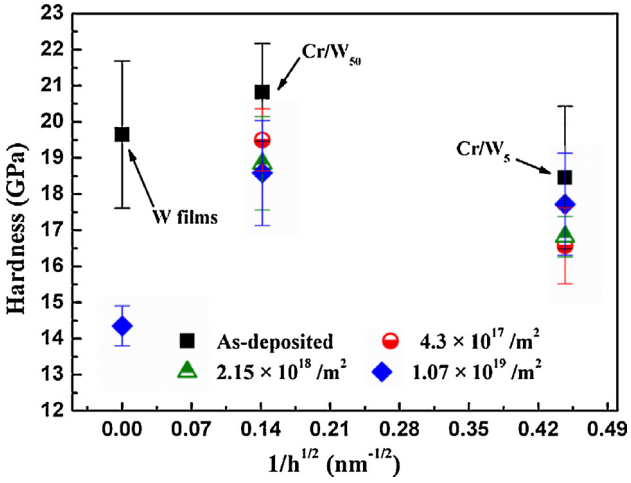

Fig. 7. Hardness evolution of the three species of thin films upon different Xe ion irradiation: horizontal ordinate in the figure is the reciprocal of square root of the modulation period of multilayer. The value of hardness and its error bar were calculated from five indentation test results.

3.3. Mechanical properties

The hardness and Young's modulus of the three species of thin films upon different Xe ions irradiation are shown in Figs. 7 and 8, respectively. Although the nano-indentation test could not provide a measurement of the actual mechanical properties of films at one depth, it can provide information about the change trends of the mechanical properties of films upon ion irradiation and give relative comparisons between the three films. In Fig. 7, the hardness of the three species of films is close. Among the three films, the

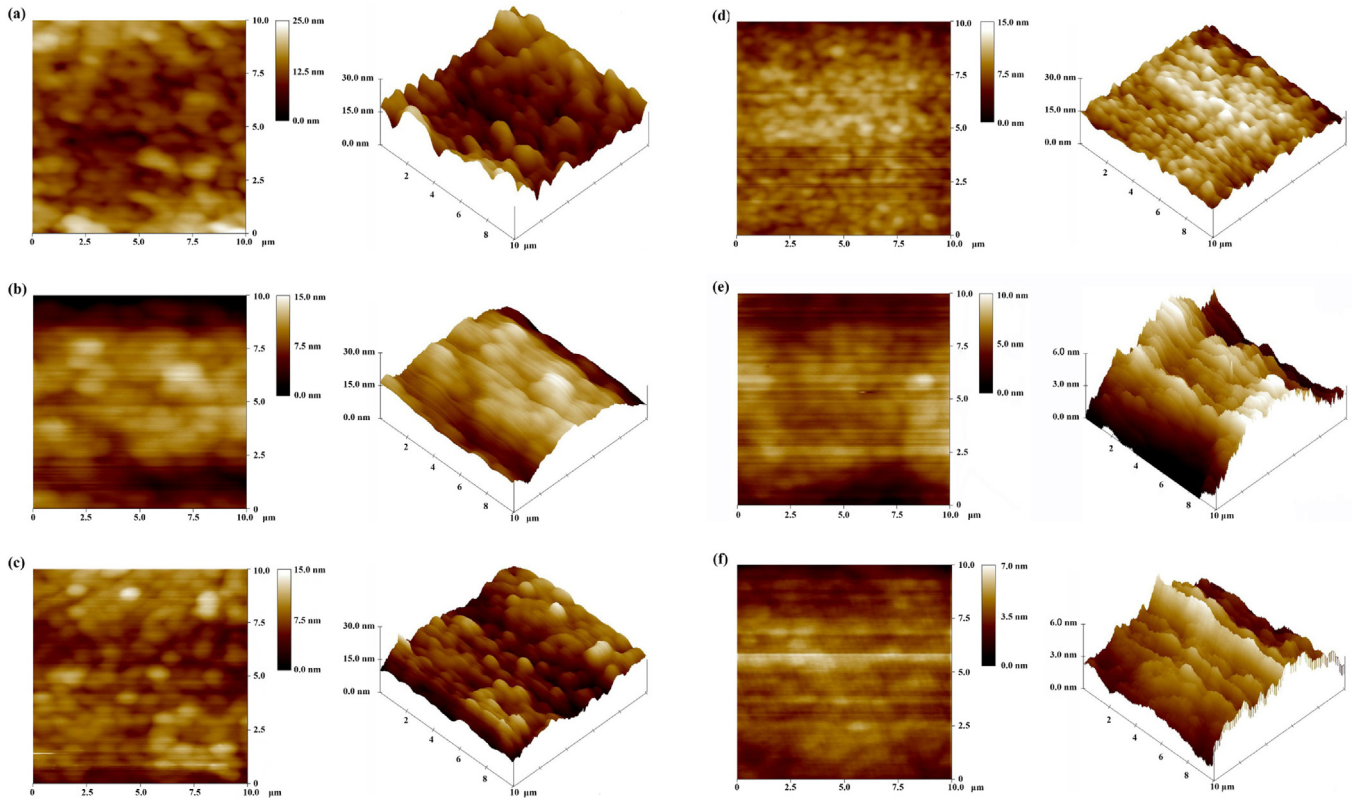

Fig. 6. AFM images of the as-deposited and post-irradiated films: (a) the as-deposited pure W film; (b) the post-irradiated pure W film; (c) the as-deposited $[Cr/W\ (50\,nm)]_2$ multilayer film; (d) the post-irradiated $[Cr/W\ (50\,nm)]_2$ multilayer film; (e) the as-deposited $[Cr/W\ (5\,nm)]_{20}$ multilayer film and (f) the post-irradiated $[Cr/W\ (5\,nm)]_{20}$ multilayer film.

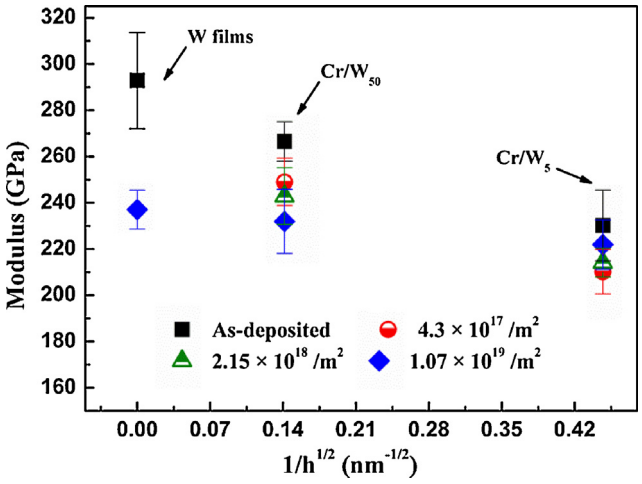

Fig. 8. Young's modulus evolution of the three species of thin films upon different Xe ion irradiation: horizontal ordinate in the figure is the reciprocal of square root of the modulation period of multilayer. The value of modulus and its error bar were calculated from five indentation test results.

$[Cr/W\ (5\,nm)]_{20}$ multilayer film is the softest. The slight decrease of hardness may be caused by the nanocrystal structure of the $[Cr/W\ (5\,nm)]_{20}$ multilayer film referred above; Latapie et al. [17] and Perne [18] have theoretically predicted and reported the grain size dependence of nano-hardness and modulus. After irradiation, the hardness of the three species of films decreases significantly. However, the hardness of the $[Cr/W\ (5\,nm)]_{20}$ multilayer film decreases at the initial stage of irradiation and gradually increase with ion irradiation fluence. When ion irradiation fluence is greater than $1.07 \times 10^{19}\ m^{-2}$, the $[Cr/W\ (5\,nm)]_{20}$ multilayer film has the least change of hardness. A similar phenomenon can be observed in the change trends of Young's modulus shown in Fig. 8.

4. Conclusion

In conclusion, a series of studies were performed on the evolution of Cr/W multilayer films' microstructure, surface morphology, and mechanical properties upon 3 MeV Xe^{20+} ions irradiation. A phase transition of tungsten from β phase (simple cubic structure) to α phase (bcc structure) can be observed in both the pure W films and two species of Cr/W multilayer films after irradiation. It seems that the multilayer structure does not work to prevent the phase transition. In addition, the nanocrystals can be observed in the as-deposited and post-irradiated $[Cr/W\ (5\,nm)]_{20}$ multilayer films.

Surface morphology characterization of pure W films showed that significant swelling effects would occur after Xe ion irradiation, however, the effect of radiation seems unconspicuous on the Cr/W multilayer films. In addition, the decrease of hardness and Young's modulus on the Cr/W multilayer films was also less than pure W films. Results of surface morphology and mechanical tests suggested that radiation tolerance of Cr/W multilayer films is significantly better than that of pure W films.

Acknowledgements

This work was funded by the Priority Academic Program Development of Jiangsu Higher Education Institutions, China Postdoctoral Science Foundation (Grant no. 2014M561642), the Jiangsu Planned Projects for Postdoctoral Research Funds (Grant no. 1401091C), the Fundamental Research Funds for the Central Universities, and the Funding of Jiangsu Innovation Program for Graduate Education and the Fundamental Research Funds for the Central Universities (CXZZ13_0159). The irradiation experimental work was performed on the 320 kV-platform for multi-discipline research, with highly charged ions at the Institute of Modern Physics, CAS. We wish to acknowledge the help of Jingyu Li, Huiping Liu, Long Kang, and Tongmin Zhang during the ion irradiation experiments.

References

[1] R.W. Grimes, R.J.M. Konings, L. Edwards, Greater tolerance for nuclear materials, Nat. Mater. 7 (2008) 683–685.
[2] G. Ackland, Controlling radiation damage, Science 327 (2010) 1587–1588.
[3] M.J. Demkowicz, Y.Q. Wang, R.G. Hoagland, O. Anderoglu, Mechanisms of He escape during implantation in CuNb multilayer composites, Nucl. Instrum. Methods Phys. Res. B: Beam Interact. Mater. At. 261 (2007) 524–528.
[4] Q.M. Wei, N. Li, N. Mara, M. Nastasi, A. Misra, Suppression of irradiation hardening in nanoscale V/Ag multilayers, Acta Mater. 59 (2011) 6331–6340.
[5] Y. Gao, T.F. Yang, J.M. Xue, S. Yan, S.Q. Zhou, Y.G. Wang, D.T.K. Kwok, P.K. Chu, Y.W. Zhang, Radiation tolerance of Cu/W multilayered nanocomposites, J. Nucl. Mater. 1 (2011) 11–15.
[6] K.F. Wei, Z.G. Wang, C.B. Liu, H. Zang, C.F. Yao, Y.B. Sheng, Y.Z. Ma, Y. Song, Z.W. Lu, Modification of Fe/Cu multilayers under 400 keV Xe^{20+} irradiation, Chin. Phys. C 32 (2008) 262–264.
[7] F.D. Chen, X.B. Tang, Y.H. Yang, H. Huang, D. Chen, Investigation of structural stability and magnetic properties of Fe/Ni multilayers irradiated by 300 keV Fe^{10+}, J. Nucl. Mater. 452 (2014) 31–36.
[8] M.J. Demkowicz, R.G. Hoagland, J.P. Hirth, Interface structure and radiation damage resistance in Cu–Nb multilayer nanocomposites, Phys. Rev. Lett. 100 (2008) 136102.
[9] R.A. Bennett, J.S. Mulley, H.A. Etman, A. Sparkes, T. Eralp, G. Held, S.A. Cavill, S.S. Dhesi, Chromium nanostructures formed by dewetting of heteroepitaxial films on W(1 1 0), Phys. Rev. B 86 (2012) 045454.
[10] A. Takeuchi, A. Inoue, Classification of bulk metallic glasses by atomic size difference, heat of mixing and period of constituent elements and its application to characterization of the main alloying element, Mater. Trans. 46 (2005) 2817–2829.
[11] Z.C. Li, Y. Teng, C.H. Chen, S. Lv, G.J. Wang, Z.J. Zhang, Effect of Xe ion irradiation on photocatalytic performance of oblique TiO_2 nanowire arrays, Appl. Surf. Sci. 327 (2015) 478–482.
[12] J.F. Ziegler, M.D. Ziegler, J.P. Biersack, SRIM – The stopping and range of ions in matter (2010), Nucl. Instrum. Methods Phys. Res. B 268 (2010) 1818–1823.
[13] R. Konings, Comprehensive Nuclear Materials, first ed., Newnes, Burlington, 2012.
[14] J. Huang, K. Xu, X.J. Gong, J.F. Wang, Y.M. Fan, J.Q. Liu, X.H. Zeng, G.Q. Ren, T.F. Zhou, H. Yang, Dislocation cross-slip in GaN single crystals under nanoindentation, Appl. Phys. Lett. 98 (2011) 221906.
[15] H.W. Wang, Y. Gao, E.G. Fu, T.F. Yang, S. Yan, J.M. Xue, P.K. Chu, Y.G. Wang, Effect of high fluence Au ion irradiation on nanocrystalline tungsten film, J. Nucl. Mater. 442 (2013) 189–194.
[16] N. Durand, K.F. Badawi, P. Goudeau, Residual stresses and microstructure in tungsten thin films analyzed by X-ray diffraction–evolution under ion irradiation, J. Appl. Phys. 80 (1996) 5021.
[17] A. Latapie, D. Farkas, Effect of grain size on the elastic properties of nanocrystalline α-iron, Scr. Mater. 48 (2003) 611–615.
[18] J. Perne, Plastic flow behavior of (Cr, Al)N hard coatings in dependence of strain rate and nanostructure, Thin Solid Films 556 (2014) 390–394.